Desalination and Water Treatment
www.deswater.com

doi: 10.5004/dwt.2021.26702

214 (2021) 302–311
February

Investigations on ultrafiltration polyethersulfone membranes modified with titanate nanotubes of various characteristics

Kacper Szymański*, Dominika Darowna, Adam Czyżewski, Paulina Sienkiewicz, Sylwia Mozia*

Faculty of Chemical Technology and Engineering, Department of Inorganic Chemical Technology and Environment Engineering, West Pomeranian University of Technology in Szczecin, Pułaskiego 10, 70 - 322 Szczecin, Poland, Tel. +48 91 449 47 30; emails: kacper.szymanski@zut.edu.pl (K. Szymański), sylwia.mozia@zut.edu.pl (S. Mozia)

Received 1 May 2020; Accepted 28 July 2020

ABSTRACT

The influence of various types of titanate nanotubes (TNTs) on the morphology, water permeability and antifouling performance of the mixed matrix polyethersulfone (PES) ultrafiltration (UF) membranes was examined. Moreover, the effect of the procedure of the dispersion of the nanomaterial (direct sonication – using ultrasonic probe vs. indirect sonication – using ultrasonic bath) in the polymer solvent on the membrane properties was determined. The membranes were prepared via wet-phase inversion using N,N-dimethylformamide as a solvent. Three types of TNTs (1 wt.% vs. PES) were applied as nanofillers: nanotubes prepared hydrothermally from Aeroxide® TiO_2 P25 (Evonik, Germany) – P25-TNTs or pure anatase (Sigma-Aldrich, USA) – A-TNTs, as well as commercially available XFJ46 (XFNANO). The membranes were characterized based on scanning electron microscopy and atomic force microscopy. Both the procedure of casting dope preparation and the TNTs morphology had an influence on the properties of the membranes. The highest resistance to fouling by bovine serum albumin exhibited the membrane prepared with application of P25-TNTs and indirect sonication. The membranes fabricated using direct sonication were characterized by the highest pure water flux. Addition of fine P25-TNTs and XFJ-TNTs was more beneficial for improvement of water permeability than incorporation of larger and thicker A-TNTs.

Keywords: Titanate nanotubes; Polyethersulfone membrane; Ultrafiltration; Bovine serum albumin; Fouling

1. Introduction

Membranes have gained an important place in chemical technology and are used in a broad range of applications. However, despite numerous advantages, one of the main drawbacks is permeate flux decline resulting from membrane fouling due to the deposition of feed components on a membrane surface and/or within its pores [1]. Hence, development of novel membranes with improved resistance to fouling plays a crucial role. The attempts focused on modification of surface properties and structure of membranes towards mitigation of fouling phenomenon are usually insufficient to solve the problem [2]. Therefore, a different approach is being developed nowadays. Namely, nanotechnology creates an opportunity to prepare membranes modified by various nanoparticles with superior

* Corresponding authors.

antifouling and hydrophilic properties [3]. The nanoparticles are incorporated into polymer membranes matrix or are deposited/immobilized on membranes surface to enhance their hydrophilicity, mechanical stability, selectivity, permeability and fouling resistance [2].

One of the most common polymers applied for microfiltration (MF) and ultrafiltration (UF) membranes fabrication is polyethersulfone (PES). However, despite several advantages such as high chemical and temperature resistance, it is characterized by a relatively low hydrophilicity. This parameter contributes to a low permeate flux and the proneness of membranes to fouling due to the enhanced attraction of hydrophobic particles and molecules to the membrane surface. Thus, numerous attempts of modification of PES membranes with various nanomaterials have been described in the subject literature. One of the most common approaches is the application of carbon nanotubes (CNTs). It was reported [4,5] that CNTs-modified PES membranes exhibited improved permeate flux and superior fouling resistance. The modifications of PES membranes with Ag and Cu nanoparticles have also been described. The results were very promising, especially in terms of (bio) fouling reduction [6]. Moreover, the PES membranes were modified with nanoparticles such as TiO_2 [7–12], SiO_2 [13], Al_2O_3 [14], ZnO [15], halloysite nanotubes [16,17] and others.

Very few reports refer, however, to the application of pure titanium (TiO_2) or titanate ($Na_xH_{2-x}Ti_2O_4(OH)_2$, $Na_xH_{2-x}Ti_3O_7$, etc.) nanotubes (TNTs) for polymeric membranes fabrication [18–22]. Similarly, the works referring to utilization of functionalized or modified TNTs are also limited [19,23–28]. Shen et al. [29] proposed the deposition of hydrothermally manufactured $Na_2Ti_3O_7$ ultralong nanotubes onto porous cellulose filter by a facile vacuum filtration to obtain the self-cleaning and photocatalytically active membranes. Another approach for fabrication of photocatalytic membranes was based on incorporation of TiO_2 nanotubes via anodization of the titanium layer sputtered onto the PES membrane surface [7,21]. TNTs were also used for modification of PES membranes dedicated to water desalination via vacuum membrane distillation [30,31] and reverse osmosis [32,33], as well as for preparation of membranes for nanofiltration [32], UF [18] and MF [7]. Shaban et al. [31] obtained TNTs-modified PES membrane for vacuum membrane distillation from a casting solution containing the polymer, 1-methyl-2-pyrrolidone (NMP) as a solvent, sodium dodecyl sulfate as dispersing agent and TNTs (0.18–0.85 wt.%) as a nanofiller. The TNTs were synthesized hydrothermally from commercial anatase TiO_2 and post-treated at 500°C for 3 h. They exhibited diameter of around 13 nm and length of about 300 nm [33]. To improve the nanofiller dispersion, the TNTs were stirred with SDS before addition to NMP and PES [31]. Gohari et al. [34] prepared PES UF membranes for adsorptive arsenate (As(V)) removal. The membranes were modified with TNTs synthesized hydrothermally from Aeroxide® TiO_2 P25 (length 250–300 nm, diameter 9–10 nm). The TNTs/PES ratio was very high and ranged from 0.125 to 1.500. The nanofiller was first dispersed in NMP containing dissolved polyvinylpyrrolidone using sonication for 12 h and subsequently the granular PES was added to the suspension under continuous stirring at 60°C. The prepared casting dope was again sonicated for 30 min and then the membrane was casted. Such obtained membranes exhibited high adsorption capacity towards As(V) (up to ca. 125 mg g^{-1}) and high water permeability (up to 1,250 L m^{-2} h^{-1} bar^{-1}), and both parameters were increasing with rising TNTs content.

Based on the above reports, two main directions of the mixed matrix membranes fabrication have been distinguished, depending on the strategy applied for NPs introduction, that is, incorporation in the membrane matrix vs. deposition onto its surface. In case of the mixed matrix membranes modified with TNTs, the mechanical mixing, especially magnetic stirring, is a widely used method of preparation of NPs dispersion in a polymer casting dope [31,35,36]. However, the main drawback of the procedure utilizing mechanical stirring is reaggregation of NPs due to the action of van der Waals forces [35]. Therefore, at various stages of preparation of the casting dope containing NPs, ultrasounds are used to counteract this unfavorable phenomenon and to improve the dispersion of the nanofiller in the membranes structure [37]. A crucial role of homogenous TNTs dispersion within polymeric membranes matrices for the enhancement of their antifouling properties and water permeability was reported previously [24].

The literature review presented above revealed also that different researchers applied various TNTs for membranes fabrication via different approaches. Direct comparison of the influence of the procedure of TNTs dispersion in polymer solvent with reference to the membrane performance is, however, impossible. Moreover, none of the published papers refers to the effect of the type of TNTs on the properties of the modified membranes. In view of the above, the aim of the present work was the investigation of the influence of the physicochemical properties of various types of titanate nanotubes (TNTs) on the morphology, water permeability and antifouling performance of the mixed matrix polyethersulfone ultrafiltration membranes. Moreover, the effect of a method of TNTs dispersion (direct vs. indirect sonication) on membranes properties was also evaluated.

2. Experimental setup

2.1. Materials

PES polymer (Veradel® 3000P, Solvay Speciality Polymers Belgium SA, Belgium) and N,N-dimethylformamide (DMF) solvent (Avantor Performance Materials Poland S.A., Poland) were used for preparation of membrane casting solution, while pure water (Elix 3, Millipore, USA) was applied as a non-solvent. TNTs were prepared hydrothermally from Aeroxide® TiO_2 P25 (Evonik, Germany) or TiO_2 anatase (Sigma-Aldrich, USA) using NaOH and HCl solutions (Avantor Performance Materials Poland S.A., Poland). The TNTs were denoted later as P25-TNTs and A-TNTs, respectively. Moreover, the commercial XFJ46 TNTs (denoted later as XFJ-TNTs) purchased from XFNANO (China) were applied. Bovine serum albumin (BSA, 66,000 g moL^{-1}; Merck Millipore, Germany) at a concentration of 1 g L^{-1} was used as a model foulant.

2.2. Preparation of TNTs

TNTs were prepared using hydrothermal method [38] in the BLH-800 pressure reactor (Berghof, Germany). First 0.5 g of TiO_2 P25 or TiO_2 anatase, and 60 mL of 10 M NaOH were added into 75 mL Teflon vessel and sonicated in an ultrasonic bath for 1 h. Then the vessel was mounted in the reactor and the hydrothermal reaction was performed for 24 h at the temperature of 140°C. Subsequently the obtained suspension was washed with ultrapure water (Simplicity®, Millipore), 0.1 M HCl and again with ultrapure water. The obtained nanomaterial was then dried (80°C for 24 h) and ground using agate mortar.

2.3. Preparation of membranes

The membranes were prepared using wet-phase inversion method. The casting solution for fabrication of the unmodified membrane (M1) was obtained by dissolution of 8.38 g of PES (15 wt.%) in 50 mL of DMF in a tightly closed bottle. Then the casting dope was degassed and casted on a glass plate using an automatic film applicator (Elcometer 4340, Elcometer Ltd., UK) with a knife (gap set at 0.1 mm). Subsequently the casted film was immersed in the pure water coagulation bath at 20°C for 24 h.

The preparation procedure of TNTs-modified membranes (1 wt.% of TNTs in relation to PES) consisted of three stages:

- *Stage 1*: Dispersion of TNTs in DMF (suspension A - SuA).
- *Stage 2*: Preparation of casting dope by addition of SuA to the solution A (SoA) containing PES in DMF.
- *Stage 3*: Casting on a glass plate and immersing in a water coagulation bath.

The suspension A (83.8 mg of TNTs in 10 mL of DMF) was prepared by sonication for 30 min using either (a) indirect method with application of an ultrasonic bath (Sonic-6D, Polsonic, Poland; output power 320 W, frequency 40 kHz) or (b) direct method utilizing an ultrasonic probe (Vibracell VCX-130, Sonics & Materials Inc., USA; output power 130 W, frequency 20 kHz, amplitude 80%). The obtained SuA was subsequently added to the solution A containing 8.38 g of PES dissolved in 40 mL of DMF and mixed for 2 h alternating between stirring at 55°C–60°C using magnetic stirrer (50 rpm) for 15 min and sonication in ultrasonic bath at 20°C–25°C for 15 min. Such prepared casting dope was casted using the automatic applicator equipped with a knife (0.1 mm gap) and then immersed in a water coagulation bath at 20°C ± 1°C for 24 h. The surface of the obtained sheets of membranes was 0.06 m^2, and their thickness measured with a micrometric screw ranged from 35 to 40 μm.

A summary of the procedures applied during preparation of the membranes is presented in Table 1.

2.4. Membrane installation

Membrane installation applied in the experiments is shown in Fig. 1. The feed was pumped from the feed tank using a plunger pump equipped with a pressure dampener into two parallel stainless steel membrane modules with manometers and needle valves. The effective (working) area of each membrane was 0.0025 m^2. The 1.194 mm feed spacers were used. The feed temperature was maintained at 20°C ± 1°C. During measurement of pure water flux (PWF), the transmembrane pressure (TMP) was set at 0.1–0.3 MPa and the feed cross-flow velocity (v) was 1 m s^{-1}. The TMP for the fouling studies was set at 0.2 MPa. The changes of the permeate flux were evaluated by measuring the volume of the permeate passing through the membrane during a fixed period of time. Each experiment was repeated at least three times in order to confirm the reproducibility of the results.

2.5. Characterization of TNTs and membranes

The specific surface area (SSA) of TNTs was assessed using the Brunauer–Emmett–Teller method with a Quadrasorb SI analyzer (Quantachrome Instruments, USA) and N_2 at 77 K as an adsorbate. Before the measurements, the samples were degassed at 100°C for 24 h under high vacuum. The phase composition of the nanotubes was evaluated based on X-ray diffraction (XRD) analysis (PANalytical Empyrean X-ray diffractometer) using CuKα radiation (λ = 1.54056 Å). The morphology of TNTs was examined with application of transmission electron microscope (TEM) FEI Tecnai F20. Before analysis, the sample was dispersed in ethanol by sonication and the obtained suspension was dropped on a

Table 1
Membranes preparation procedures

Procedure			Unmodified	Modified			
			M1	M2	M3	M4	M5
			–	P25-TNTs	P25-TNTs	A-TNTs	XFJ-TNTs
Stage 1	SuA (TNTs + DMF)	Ultrasonic bath	–	0.5 h	–	–	–
		Ultrasonic probe	–	–	0.5 h	0.5 h	0.5 h
Stage 2	SuA + SoA (PES + DMF + TNTs)	Stirring (55°C–60°C; 15 min) + sonication (20°C–25°C; 15 min) – by turns	–	2 h	2 h	2 h	2 h
Stage 3: casting							

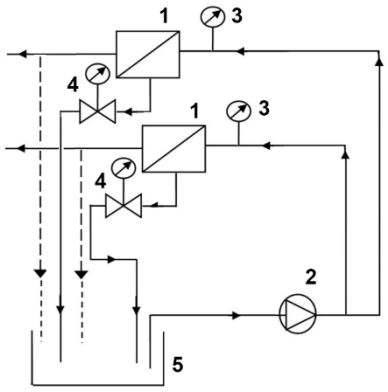

Fig. 1. Schematic diagram of membrane installation utilizing ultrafiltration. 1 – membrane modules, 2 – plunger pump, 3 – manometers, 4 – needle valves with manometers, 5 – feed tank.

copper grid (300 mesh). The isoelectric point (pH(I)) of the TNTs was measured with application of Zetasizer Nano-ZS (Malvern Instruments Ltd., Great Britain) equipped with Multipurpose Titrator MPT-2 and a degasser. Before measurement, the NPs were dispersed in ultrapure water and the pH was adjusted using HCl and NaOH solutions.

The surface morphology of the membranes was investigated using atomic force microscopy (AFM) with application of NanoScope V Multimode 8 scanning probe microscope (Bruker Corp., USA). The measurements were performed with the silicon nitride ScanAsyst-Air probe in the ScanAsyst mode, which uses the so-called PeakForce Tapping Mechanism. The scanned area was 10 μm × 10 μm. The cross-section of the obtained membranes was examined using Hitachi SU8020 Ultra-High-Resolution Field Emission Scanning Electron Microscope (UHR FE-SEM). Before analysis, the samples of the membranes were soaked in ethanol–water and ethanol solutions to keep the structure unchanged and subsequently broken in liquid nitrogen and sputtered with Cr under vacuum. Hydrophilic properties of the prepared membranes were determined based on water contact angle measurements performed with the use of a goniometer (Surface Energy Evaluation System, Advex Instruments, Czech Republic). The contact angle values were calculated as an average of at least 10 measurements from 5 different membrane pieces. The antifouling performance of the membranes was evaluated during ultrafiltration of BSA solution. The fouling resistance (R_f) was calculated as a difference between the total resistance of the fouled membrane (R_t) and the resistance of the clean membrane (R_m) according to the resistance-in-series approach using the following equations:

$$R_f = R_t - R_m \tag{1}$$

$$R_m = \frac{\mathrm{TMP}}{\mathrm{PWF}\cdot\eta} \tag{2}$$

$$R_t = \frac{\mathrm{TMP}}{J\cdot\eta} \tag{3}$$

where J – permeate flux during UF of BSA solution, η – viscosity.

The concentration of BSA in feed and permeate was determined using the total organic carbon measurements (multi N/C 3100 analyzer, Analytik Jena, Germany). The rejection coefficient was calculated on the basis of Eq. (4):

$$R(\%) = \left(1 - \frac{c_{\mathrm{permeate}}}{c_{\mathrm{feed}}}\right)\cdot 100\% \tag{4}$$

where c_{permeate} and c_{feed} represent the concentrations of BSA in permeate and feed, respectively.

3. Results and discussion

3.1. Physicochemical properties of TNTs

The morphology of the applied TNTs was investigated with the use of transmission electron microscopy. In case of TNTs obtained from TiO_2 P25, the mean values of outer diameter and length were 9(2) nm and 78(25) nm, respectively (Fig. 2a). TNTs from anatase (Fig. 2b) exhibited mean diameter of 13(3) nm and length of 188(41) nm, while XFJ-TNTs had diameter and length of ca. 10(2) and 61(20) nm, respectively (Fig. 2c).

The XRD patterns of the prepared nanotubes (Fig. 3) exhibited three peaks positioned at 2θ angle of ca. 24.5° (110), 28.5° (211) and 48.5° (020), which could be ascribed to the $A_2Ti_2O_5{\cdot}H_2O$, $A_2Ti_3O_7$, and lepidocrocite titanates [39,40].

All the TNTs were characterized by a well-developed surface area, and the SSA reached 250 and 277 $m^2\,g^{-1}$ for XFJ-TNTs and A-TNTs, respectively. Significantly larger SSA was noted in case of P25-TNTs (322 $m^2\,g^{-1}$). The differences can be attributed to the visibly higher volume of micropores measured for P25-TNTs (0.11 $cm^3\,g^{-1}$) compared with XFJ-TNTs (0.088 $cm^3\,g^{-1}$) and A-TNTs (0.097 $cm^3\,g^{-1}$). The total pore volume of P25-TNTs was similar to that determined for A-TNTs (1.4 $cm^3\,g^{-1}$), while the value measured in case of XFJ-TNTs was slightly higher (1.6 $cm^3\,g^{-1}$).

The TNTs were characterized by various values of the isoelectric point pH(I). This parameter defines the pH at which the NPs surface carries no net electrical charge, meaning that the positive and negative charges cancel out. Above pH(I), the surface of the nanotubes is negatively charged while below the isoelectric point it is positively charged. The lowest pH(I) was observed in case of A-TNTs (3.1). The isoelectric point of P25-TNTs was 3.4, while that of XFJ-TNTs amounted to 3.9.

The results discussed above show that the TNTs applied in the investigations exhibited different morphology, porosity and surface charge. Therefore, it was postulated that their effect on the properties of the mixed-matrix membranes could also be different.

3.2. Physicochemical properties of membranes

To evaluate the influence of the TNTs dispersion procedure and the TNTs type on the morphology of the modified membranes, the SEM observations were realized. The results are presented in Fig. 4. All the membranes were

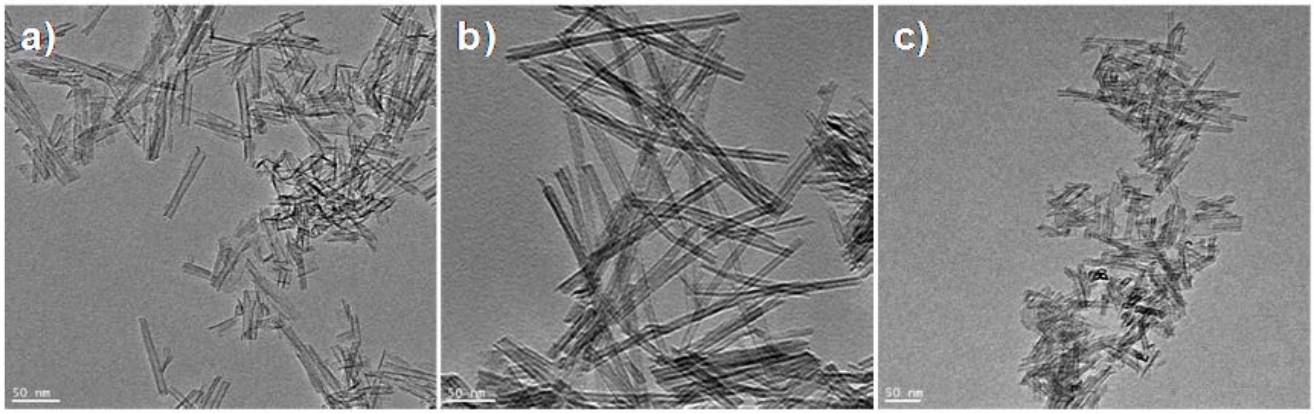

Fig. 2. Transmission electron microscope images of the TNTs applied for membranes modification: (a) P25-TNTs, (b) A-TNTs, and (c) XFJ-TNTs.

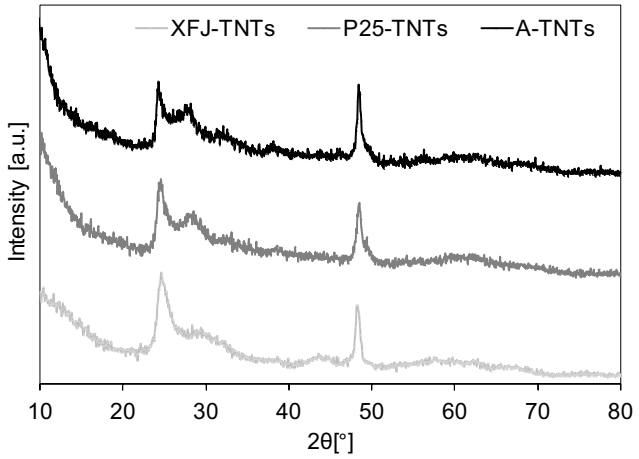

Fig. 3. XRD patterns of TNTs.

asymmetric with a thin skin layer and a porous support layer containing finger-like pores and a spongy structure between them. Moreover, some oval macrovoids can be observed in the bottom part of the cross sections.

The microphotographs of the membranes prepared under various TNTs sonication conditions (M2 and M3) revealed significant differences in size and distribution of TNTs agglomerates in the polymer matrix. The application of indirect sonication (using ultrasonic bath) resulted in formation of larger TNTs agglomerates compared with the direct method (i.e., with the use of ultrasonic probe). The mean size of the agglomerates calculated on the basis of SEM analysis amounted to ca. 5.4(4.4) μm in case of M2 and ca. 2.3(1.3) μm in case of M3. These data confirm the superior effect of sonication by the direct approach. Application of a probe allows to obtain a more efficient cavitation in the TNTs suspension in DMF, due to focusing of the ultrasound energy in a localized sample zone. In case of the indirect sonication, the ultrasonic waves first need to pass the liquid inside the ultrasonic bath, then cross the wall of the sample container and after that reach the suspension. Thus, the efficiency of the process is lower [41,42].

Fig. 4 presents also a comparison of the cross sections of membranes prepared under the same sonication conditions but containing various type TNTs (M3-M5). The finest TNT agglomerates were observed in case of M5 membrane (mean size of ca. 1.3 μm), while the mean diameter of the structures found in M4 membrane was similar to that observed in M3 (ca. 2.1–2.3 μm). These data are in agreement with the dimensions of various TNTs calculated on the basis of TEM analysis (Fig. 2). The XFJ-TNTs were characterized by the shortest length (61(20) nm), which resulted in formation of the smallest aggregates. The dimensions of P25-TNTs and A-TNTs were larger (78(25) nm and 188(41) nm, respectively) leading to formation of larger agglomerates. In case of all membranes, the presence of TNTs was observed in various parts of the cross section.

The results presented in Fig. 4 revealed that both the procedure of TNTs dispersion and the type of TNTs have an influence on the morphology of the membranes. In the next stage of the research, the topography of the membranes surface was also analyzed in detail. Fig. 5 shows the AFM images of the obtained membranes. The differences in the distribution of the TNTs are clearly visible. On the surface of the M2 membrane prepared under gentle sonication, the large agglomerates of TNTs were present along with some small convex formations, confirming the high non-uniformity of the nanofiller dispersion. In case of the M3 membrane, fabricated using the direct sonication of TNTs suspension, the NPs agglomerates are also visible; however, their diameters are significantly lower compared with those observed for M2. Moreover, some fine needle-like structures are present. These observations revealed that the direct method of TNTs dispersion was more effective in the NPs deagglomeration compared with the indirect approach. The membranes prepared under the same direct sonication conditions, but containing various type TNTs (M3-M5) exhibited some differences in their topography. The agglomerates of the nanotubes observed for M5 membrane, modified with XFJ-TNTs, were smaller compared with the M3 and M4 membranes. Nevertheless, for all of the membranes, the presence of the needle-like structures was noted. The obtained results are well reflected in the TNTs

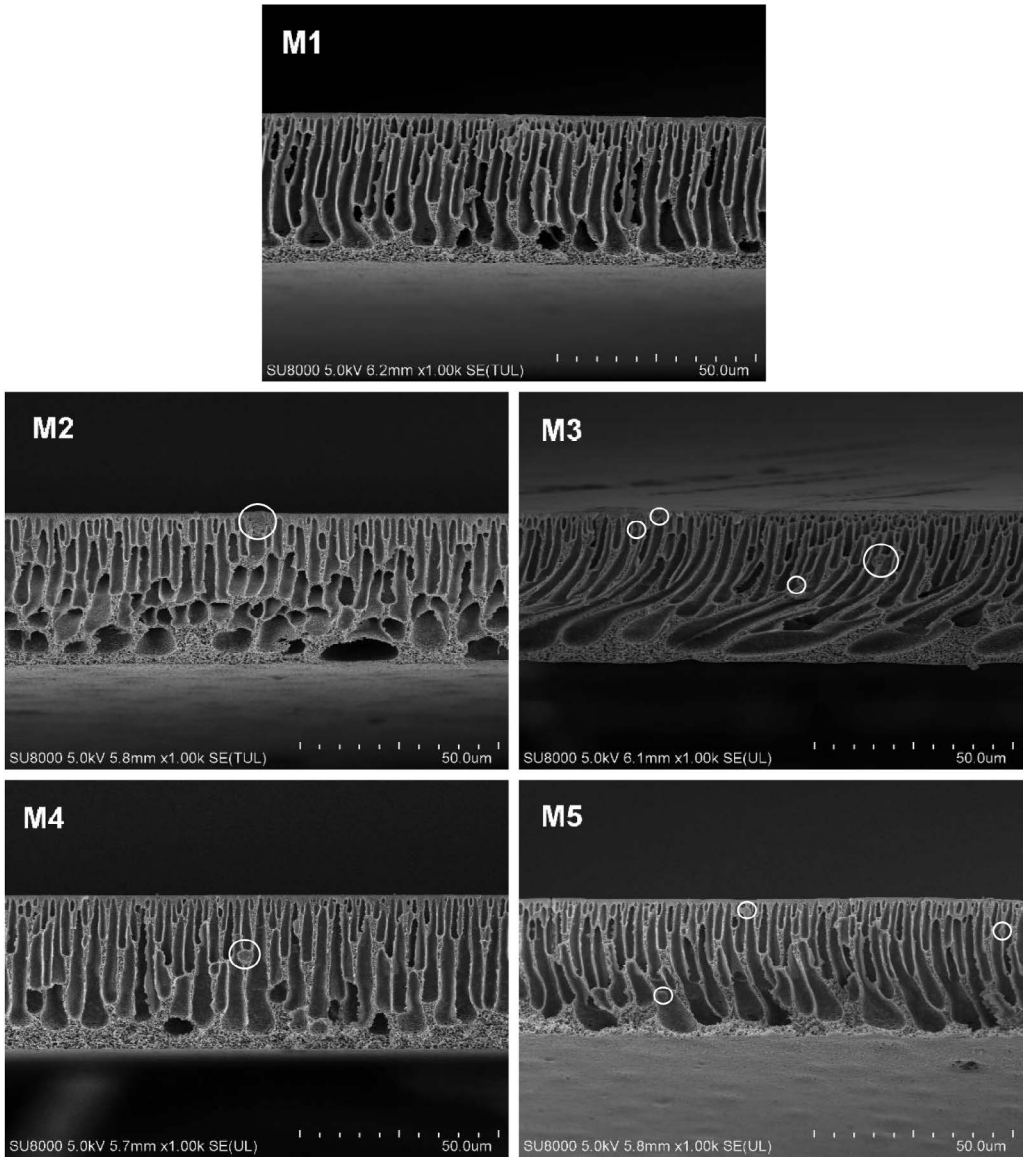

Fig. 4. SEM cross-sections of the unmodified membrane M1 and the modified M2–M5 membranes. TNTs agglomerates are marked with circles.

dimensions (Fig. 2) showing that the finest NPs agglomerates were formed when the smallest XFJ-TNTs were applied.

The mean surface roughness (R_a) values calculated on the basis of the AFM images revealed that all the mixed-matrix membranes exhibited more rougher surface than the unmodified one (R_a of M1 was 4.9(0.8) nm). The roughness of the M3 membrane, prepared according to the procedure utilizing direct sonication, was higher (11.6(6.0) nm) compared with R_a of the M2 membrane fabricated with application of ultrasonic bath (9.6(2.0) nm). These results are in compliance with the aforementioned results of SEM analysis. Namely, poor dispersion of TNTs in case of the application of the indirect sonication caused formation of larger aggregates, which remained below the membrane skin, as can be observed in Fig. 5. The number of the needle-like structures contributing to the increase of R_a was in case of M2 very limited. The surface roughness of the membranes modified with various TNTs utilizing direct sonication followed the order: XFJ-TNTs (13.5(4.7) nm) > P25-TNTs (11.6(6.0) nm) > A-TNTs (9.8(2.3) nm). These data suggest that application of TNTs with smaller dimensions could lead to formation of a more rougher surface.

3.3. Transport properties of membranes PWF

Fig. 6 presents mean values of permeate fluxes measured during ultrafiltration of pure water. A linear dependence between PWF and TMP was observed for all the examined membranes. The lowest permeate fluxes were noted in case of the unmodified M1. The addition of TNTs resulted in a significant improvement of PWF in case of all the mixed matrix membranes. Nonetheless, both the TNTs dispersion

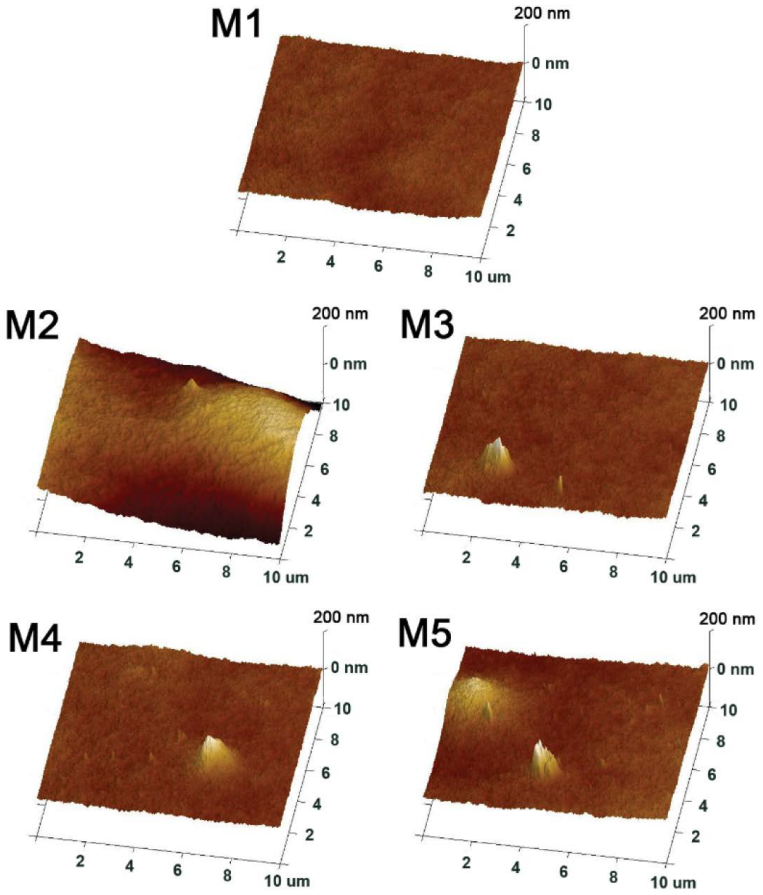

Fig. 5. AFM images of the prepared membranes.

procedure and the type of the NPs affected the water permeability of the membranes. The lowest increase of PWF was found in case of the M2 membrane, for which the flux measured at 0.3 MPa was higher for only ca. 12% compared with M1. Under the same conditions, the PWF value determined for M3, also containing TNTs-P25 but dispersed using ultrasonic probe, was higher compared with M1 for about 38%. The increase of PWF in case of M4 and M5 membranes reached ca. 16% and ca. 31%, respectively.

The data presented in Fig. 6 revealed that the membrane prepared using direct sonication of TNTs (M3) exhibited higher permeability than the one prepared with application of the indirect method (M2). These results are in agreement with AFM and SEM analyses and can be attributed mainly to the improved dispersion of TNTs within the membranes structure (Figs. 4 and 5). The importance of good TNTs dispersion for water permeability of the modified membranes was also underlined by Ng et al. [24]. Moreover, it was confirmed that the type of TNTs had a significant impact on the membrane performance (Fig. 6). The most beneficial effect in terms of water permeability improvement was obtained upon addition of P25-TNTs and XFJ-TNTs. The increase of permeability can be attributed to the presence of a larger number of pores formed in the PES matrix due to the action of nanotubes at the stage of phase inversion process as well as to the additional pores formed by the TNTs themselves.

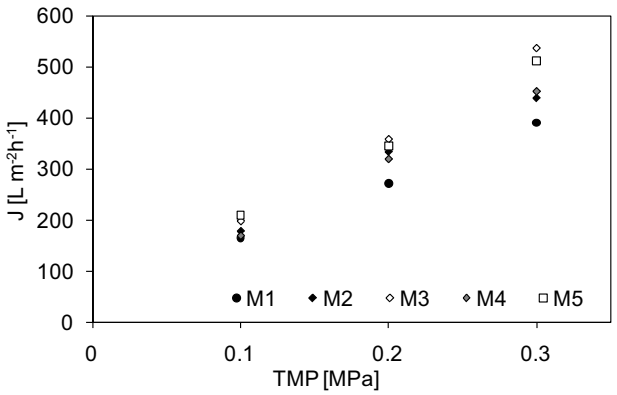

Fig. 6. Effect of TMP on the pure water flux through M1–M5 membranes.

That results from the open-ended nanotubular morphology of the TNTs and could be affected by the structural properties of the nanotubes. The data summarized in Fig. 6 suggest that the application of short nanotubes such as P25-TNTs and XFJ-TNTs could lead to the formation of a greater number of pores within membrane than in case of longer and thicker A-TNTs. Additionally, the M3 membrane exhibited slightly higher hydrophilicity (water contact angle: 51°) than M4

(54°), which could affect the adsorption of water molecules and thus water permeation through the membranes.

3.4. Investigations on permeate flux during ultrafiltration of BSA solution

In order to evaluate the antifouling properties of the prepared membranes, a series of experiments with the application of bovine serum albumin was carried out. Fig. 7 shows the permeate fluxes (J) during ultrafiltration of BSA solution through the unmodified M1 membrane and the membranes modified with TNTs (M2-M5). For all of the tested membranes, the decrease of permeate flux was observed from the beginning of the process and the highest decline was found during the initial 30 min of experiment. After that, the flux started to stabilize. Such course of the flux changes results from the mechanism of membrane fouling by BSA. The albumin molecules are attracted easily by the negatively charged surfaces of the membranes. The force of BSA-membrane adhesion is the strongest at the very beginning of the fouling, which corresponds to the highest decline of permeate flux (Fig. 7) [43]. At this stage, a very thin and uniform layer of albumin molecules is formed on the surface of membranes. The fouled membranes change their surface charge to more positive values, which weakens the attraction of BSA. Due to a simultaneous repulsive force experienced by the neighboring BSA molecules and a membrane surface, the formed gel layer exhibits lesser tendency to compress [44]. As a result, the stabilization of permeate flux is observed, similarly as that presented in Fig. 7.

From the results summarized in Fig. 7, it can be also found that the lowest permeate flux values were measured for the unmodified membrane (M1), that is, 124 L m^{-2} h^{-1} at the end of the process. The highest flux was found in case of M2 modified with TNTs-P25 dispersed using ultrasonic bath (170 L m^{-2} h^{-1} after 120 min). The flux measured for M3, also modified with TNTs-P25, but dispersed with application of the ultrasonic probe, was lower and amounted to 153 L m^{-2} h^{-1}. These data show that the effect of the TNTs dispersion procedure in case of BSA fouling was opposite to that observed for PWF. One explanation can be that fouling is a flux-dependent phenomenon [45] and therefore the decrease of permeate flux noted for M2, which was characterized by lower PWF than M3 (Fig. 6), was also less severe. A higher surface concentration of BSA molecules being a result of improved mass transfer caused by a higher permeability of M3, led to its stronger fouling [45].

The permeate flux after 120 min of ultrafiltration of BSA solution through M4 and M5 membranes was slightly lower compared with M3 and reached 142 and 129 L m^{-2} h^{-1}, respectively. These results confirm that the type of TNTs had an influence not only on membranes permeability but also on their proneness to fouling. The highest value of fouling resistance (R_f) was noted for M1 (unmodified) and M5 membranes (4.1×10^{12} m^{-1} and 3.7×10^{12} m^{-1}, respectively), in which cases the deterioration of permeate flux compared with PWF was the highest (70%). The fouling resistance calculated for M3 and M4 membranes was similar to each other and amounted to 3.1×10^{12} m^{-1}. The lowest R_f value was observed for the M2 (2.3×10^{12} m^{-1}), which corresponded with the lowest permeate flux deterioration

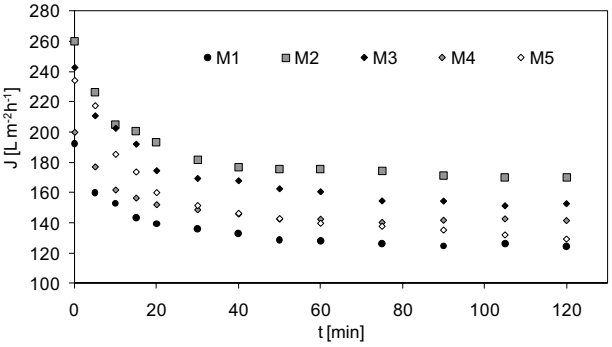

Fig. 7. Permeate fluxes during ultrafiltration of BSA solution for different kind of membranes.

during UF of BSA through that membrane compared with PWF (54%). Analyzing the value of permeate flux J at the end of the experiment with reference to pure water flux, the following order was observed for the mixed-matrix membranes: M2 < M4 < M3 < M5. This order confirms the importance of the permeability of the membranes, which was discussed above. The M4 membrane was characterized by lower PWF than M3 and M5 and, therefore, was also slightly less fouled. Moreover, the order presented above is the same as that observed for the R_a values, which increased as follows: M2 (9.6 nm) < M4 (9.8 nm) < M3 (11.6 nm) < M5 (13.5 nm). Thus, another explanation for the observed differences in the severity of membrane fouling can be surface roughness. The rougher surface could promote adsorption of BSA molecules, which results in fouling intensification.

The obtained results clearly show that both the physicochemical characteristics of TNTs and their dispersion within membrane matrix have significant influence on the membrane fouling by BSA. Although all the mixed-matrix membranes exhibited improved resistance to fouling, the highest permeate flux was found in case of the M2 and M3 membranes containing TNTs-P25. Nonetheless, the permeate flux decline was the least severe in case of the M2 sample, despite it contained larger TNTs agglomerates than M3. These results can be attributed to the lower water permeability of the former membrane compared with the latter one as well as to its lower roughness.

No influence of the TNTs type and distribution on the BSA separation by the modified membranes was found. The rejection coefficient (R%) in case of all the mixed-matrix membranes was 99.5%, which was slightly higher compared with that determined for the unmodified M1 (99.0%).

4. Conclusions

The influence of the presence of various TNTs and methods of their dispersion on the physicochemical, transport and antifouling properties of the polyethersulfone ultrafiltration membranes has been presented and discussed. The AFM and SEM analyses revealed that the direct sonication with the use of ultrasonic probe during the dispersion of the TNTs in DMF helped to create smaller aggregates of the NPs and allowed to distribute them more uniformly in the membrane matrix than the indirect method

with application of the ultrasonic bath. The improved dispersion of the NPs resulted in an increase of PWF, as was observed in case of M2 and M3 membranes modified with P25-TNTs. Moreover, it was found that application of fine TNTs, such as P25-TNTs and XFJ-TNTs, was more beneficial in terms of improvement of water permeability than incorporation of larger and thicker A-TNTs. That was explained in terms of formation of additional pores in the membranes structure. The modification of PES membrane with TNTs improved its resistance to fouling. The best antifouling performance exhibited the membranes modified with P25-TNTs. The decline of the permeate flux during UF of BSA solution was the least severe in case of M2 membrane characterized by the lowest water permeability and surface roughness. These data show that the effect of various TNTs on water permeability and fouling resistance of the membranes was opposite. Based on the obtained results, it was concluded that both the procedure of casting dope preparation and the morphology of the TNTs have significant influence on membranes properties and performance.

Acknowledgments

This work was supported by the National Science Centre, Poland under project No. 2016/21/B/ST8/00317.

The authors would like to thank Solvay Polska Sp. z.o.o. for providing PES samples. They would also like to express their appreciation to Dr. Karolina Szymańska for assistance with TEM measurements, Dr. Ewelina Kusiak-Nejman for assistance with N_2 adsorption–desorption measurements, Mr. Michał Zgrzebnicki for assistance with scanning electron microscope measurements and Mr. Marcin Sadłowski for assistance with X-ray diffraction measurements.

Abbreviations

η	—	Viscosity
AFM	—	Atomic force microscope
A-TNTs	—	Titanate nanotubes prepared from TiO_2 anatase
BSA	—	Bovine serum albumin
c_{feed}	—	Concentration of BSA in feed
CNTs	—	Carbon nanotubes
$c_{permeate}$	—	Concentration of BSA in permeate
DMF	—	Dimethylformamide
J	—	Permeate flux
MF	—	Microfiltration
NMP	—	1-Methyl-2-pyrrolidone (N-methylpyrrolidone)
NPs	—	Nanoparticles
P25-TNTs	—	Titanate nanotubes prepared from TiO_2 P25
PES	—	Polyethersulfone
pH(I)	—	Isoelectric point
PWF	—	Pure water flux
R(%)	—	Rejection coefficient
R_a	—	Surface roughness
R_f	—	Fouling resistance
R_m	—	Resistance of clean membrane
R_t	—	Total resistance of the fouled membrane
SDS	—	Sodium dodecyl sulfate
SoA	—	Solution A
SSA	—	Specific surface area
SuA	—	Suspension A
TEM	—	Transmission electron microscope
TMP	—	Transmembrane pressure
TNTs	—	Titanate nanotubes
UF	—	Ultrafiltration
UHR FE-SEM	—	Ultra-high-resolution field emission scanning electron microscope
v	—	Feed cross-flow velocity
XFJ46	—	Commercially available titanate nanotubes
XRD	—	X-ray diffraction

References

[1] S. Mozia, Photocatalytic membrane reactors (PMRs) in water and wastewater treatment. A review, Sep. Purif. Technol., 73 (2010) 71–91.
[2] J. Kim, B. Van der Bruggen, The use of nanoparticles in polymeric and ceramic membrane structures: review of manufacturing procedures and performance improvement for water treatment, Environ. Pollut., 158 (2010) 2335–2349.
[3] W.-Y. Wang, J.-Y. Shi, J.-L. Wang, Y.-L. Li, N.-N. Gao, Z.-X. Liu, W.-T. Lian, Preparation and characterization of PEG-*g*-MWCNTs/PSf nano-hybrid membranes with hydrophilicity and antifouling properties, RSC Adv., 103 (2015) 84746–84753.
[4] E. Celik, H. Park, H. Choi, H. Choi, Carbon nanotube blended polyethersulfone membranes for fouling control in water treatment, Water Res., 45 (2011) 274–282.
[5] N. Phao, E.N. Nxumalo, B.B. Mamba, S.D. Mhlanga, A nitrogen-doped carbon nanotube enhanced polyethersulfone membrane system for water treatment, Phys. Chem. Earth, 66 (2013) 148–156.
[6] M.C. Cruz, G. Ruano, M. Wolf, D. Hecker, E.C. Vidaurre, R. Schmittgens, V. Beatriz Rajal, Plasma deposition of silver nanoparticles on ultrafiltration membranes: antibacterial and anti-biofouling properties, Chem. Eng. Res. Des., 94 (2015) 524–537.
[7] K. Fischer, M. Kuhnert, R. Gläser, A. Schulze, Photocatalytic degradation and toxicity evaluation of diclofenac by nanotubular titanium dioxide–PES membrane in a static and continuous setup, RSC Adv., 5 (2015) 16340–16348.
[8] M.-L. Luo, J.-Q. Zhao, W. Tang, C.-S. Pu, Hydrophilic modification of poly(ether sulfone) ultrafiltration membrane surface by self-assembly of TiO_2 nanoparticles, Appl. Surf. Sci., 249 (2005) 76–84.
[9] A. Rahimpour, S.S. Madaeni, A.H. Taheri, Y. Mansourpanah, Coupling TiO_2 nanoparticles with UV irradiation for modification of polyethersulfone ultrafiltration membranes, J. Membr. Sci., 313 (2008) 158–169.
[10] A. Razmjou, J. Mansouri, V. Chen, The effects of mechanical and chemical modification of TiO_2 nanoparticles on the surface chemistry, structure and fouling performance of PES ultrafiltration membranes, J. Membr. Sci., 378 (2011) 73–84.
[11] M.L. Luo, Q.Z. Wen, J.L. Liu, H.J. Liu, Z.L. Jia, Fabrication of SPES/nano-TiO_2 composite ultrafiltration membrane and its anti-fouling mechanism, Chin. J. Chem. Eng., 19 (2011) 45–51.
[12] V. Vatanpour, S.S. Madaeni, A.R. Khataee, E. Salehi, S. Zinadini, H.A. Monfared, TiO_2 embedded mixed matrix PES nanocomposite membranes: influence of different sizes and types of nanoparticles on antifouling and performance, Desalination, 292 (2012) 19–29.
[13] J. Huang, K.S. Zhang, K. Wang, Z.L. Xie, B. Ladewig, H.T. Wang, Fabrication of polyethersulfone-mesoporous silica nanocomposite ultrafiltration membranes with antifouling properties, J. Membr. Sci., 423 (2012) 362–370.
[14] M. Homayoonfal, M.R. Mehrnia, S. Rahmani, Y.M. Mojtahedi, Fabrication of alumina/polysulfone nanocomposite

membranes with biofouling mitigation approach in membrane bioreactors, J. Ind. Eng. Chem., 22 (2015) 357–367.
[15] H. Isawi, M.H. El-Sayed, X. Feng, H. Shawky, M.S. Abdel Mottaleb, Surface nanostructuring of thin film composite membranes via grafting polymerization and incorporation of ZnO nanoparticles, Appl. Surf. Sci., 385 (2016) 268–281.
[16] Y.F. Chen, Y.T. Zhang, H.Q. Zhang, J.D. Liu, C.H. Song, Biofouling control of halloysite nanotubes-decorated polyethersulfone ultrafiltration membrane modified with chitosan-silver nanoparticles, Chem. Eng. J., 228 (2013) 12–20.
[17] S. Mozia, A. Grylewicz, M. Zgrzebnicki, D. Darowna, A. Czyżewski, Investigations on the properties and performance of mixed-matrix polyethersulfone membranes modified with halloysite nanotubes, Polymers, 11 (2019) 671–689.
[18] M.H.D.A. Farahani, H. Rabiee, V. Vatanpour, Comparing the effect of incorporation of various nanoparticulate on the performance and antifouling properties of polyethersulfone nanocomposite membranes, J. Water Process Eng., 27 (2019) 47–57.
[19] N. Mahdi, P. Kumar, A. Goswami, B. Perdicakis, K. Shankar, M. Sadrzadeh, Robust polymer nanocomposite membranes incorporating discrete TiO_2 nanotubes for water treatment, Nanomaterials, 9 (2019) 1186–1204.
[20] G.G. Liu, K. Han, H.Q. Ye, C.Y. Zhu, Y.P. Gao, Y. Liu, Y.H. Zhou, Graphene oxide/triethanolamine modified titanate nanowires as photocatalytic membrane for water treatment, Chem. Eng. J., 320 (2017) 74–80.
[21] K. Fischer, R. Gläser, A. Schulze, Nanoneedle and nanotubular titanium dioxide – PES mixed matrix membrane for photocatalysis, Appl. Catal., B, 160 (2014) 456–464.
[22] S.P. Albu, A. Ghicov, J.M. Macak, R. Hahn, P. Schmuki, Self-organized, free-standing TiO_2 nanotube membrane for flow-through photocatalytic applications, Nano Lett., 7 (2007) 1286–1289.
[23] Q. Li, H. Zhang, Z.K. Tu, J. Yu, C.X. Xiong, M. Pan, Impregnation of amine-tailored titanate nanotubes in polymer electrolyte membranes, J. Membr. Sci., 423 (2012) 284–292.
[24] Z.-C. Ng, C.-Y. Chong, W.-J. Lau, M. Karaman, A.F. Ismail, Boron removal and antifouling properties of thin-film nanocomposite membrane incorporating PECVD-modified titanate nanotubes, J. Chem. Technol. Biotechnol., 94 (2019) 2772–2782.
[25] S. Mozia, M. Jose, P. Sienkiewicz, K. Szymański, D. Darowna, M. Zgrzebnicki, A. Markowska-Szczupak, Polyethersulfone ultrafiltration membranes modified with hybrid Ag/titanate nanotubes: physicochemical characteristics, antimicrobial properties, and fouling resistance, Desal. Water Treat., 128 (2018) 106–118.
[26] S. Mozia, P. Sienkiewicz, K. Szymański, M. Zgrzebnicki, D. Darowna, A. Czyżewski, A.W. Morawski, Influence of Ag/titanate nanotubes on physicochemical, antifouling and antimicrobial properties of mixed-matrix polyethersulfone ultrafiltration membranes, J. Chem. Technol. Biotechnol., 94 (2019) 2497–2511.
[27] K. Szymański, D. Darowna, P. Sienkiewicz, M. Jose, K. Szymańska, M. Zgrzebnicki, S. Mozia, Novel polyethersulfone ultrafiltration membranes modified with Cu/titanate nanotubes, J. Water Process Eng., 33 (2020) 101098–101109.
[28] V.R. Pereira, A.M. Isloor, A.K. Zulhairun, M.N. Subramaniam, W.J. Lau, A.F. Ismail, Preparation of polysulfone-based PANI–TiO_2 nanocomposite hollow fiber membranes for industrial dye rejection applications, RSC Adv., 6 (2016) 99764–99773.
[29] S. Shen, C. Wang, M.Q. Sun, M.M. Jia, Z.H. Tang, J.H. Yang, Free-standing sodium titanate ultralong nanotube membrane with oil-water separation, self-cleaning, and photocatalysis properties, Nanoscale Res. Lett., 15 (2020) 22.
[30] H. Abdallah, A.F. Moustafa, A.A. Al Anezi, H.E. El-Sayed, Performance of a newly developed titanium oxide nanotubes/polyethersulfone blend membrane for water desalination using vacuum membrane distillation, Desalination, 346 (2014) 30–36.
[31] M. Shaban, H. AbdAllah, L. Said, H.S. Hamdy, A.A. Khalek, Titanium dioxide nanotubes embedded mixed matrix PES membranes characterization and membrane performance, Chem. Eng. Res. Des., 95 (2015) 307–316.
[32] M. Shaban, H. AbdAllah, L. Said, A.M. Ahmed, Water desalination and dyes separation from industrial wastewater by PES/TiO_2NTs mixed matrix membranes, J. Polym. Res., 26 (2019) 181.
[33] M. Shaban, H. AbdAllah, L. Said, H.S. Hamdy, A. Abdel Khalek, Fabrication of PES/TiO_2 nanotubes reverse osmosis (RO) membranes, J. Chem. Acta, 2 (2013) 59–61.
[34] R.J. Gohari, W.J. Lau, E. Halakoo, A.F. Ismail, F. Korminouri, T. Matsuura, M.S.J. Gohari, N.K. Chowdhury, Arsenate removal from contaminated water by a highly adsorptive nanocomposite ultrafiltration membrane, New J. Chem., 39 (2015) 8263–8272.
[35] C.-C. Jiang, Y.-K. Cao, G.-Y. Xiao, R.-F. Zhu, Y.-P. Lu, A review on the application of inorganic nanoparticles in chemical surface coatings on metallic substrates, RSC Adv., 7 (2017) 7531–7539.
[36] L.A. Shah, T. Malik, M. Siddiq, A. Haleem, M. Sayed, A. Naeem, TiO_2 nanotubes doped poly(vinylidene fluoride) polymer membranes (PVDF/TNT) for efficient photocatalytic degradation of brilliant green dye, J. Environ. Chem. Eng., 7 (2019) 103291–103302.
[37] S.A. Hashemifard, A.F. Ismail, T. Matsuura, Mixed matrix membrane incorporated with large pore size halloysite nanotubes (HNT) as filler for gas separation: experimental, J. Colloid Interface Sci., 359 (2011) 359–370.
[38] T. Kasuga, M. Hiramatsu, A. Hoson, T. Sekino, K. Niihara, Formation of titanium oxide nanotube, Langmuir, 14 (1998) 3160–3163.
[39] S. Preda, M. Rutar, P. Umek, M. Zaharescu, A study of thermal properties of sodium titanate nanotubes synthesized by microwave-assisted hydrothermal method, Mater. Res. Bull., 71 (2015) 98–105.
[40] G.R. Lima, W. Formentin Monteiro, R. Ligabue, R.M. Campomanes Santana, Titanate nanotubes as new nanostrutured catalyst for depolymerization of PET by glycolysis reaction, Mater. Res., 20 (2017) 588–595.
[41] M. Güney, A. Elik, Comparison of probe with bath ultrasonic leaching procedures for preparation to heavy metal analysis of bio-collectors prior to atomic absorption spectrometry, Commun. Soil Sci. Plant Anal., 48 (2017) 1741–1752.
[42] H.M. Santos, C. Lodeiro, J.-L. Capelo-Martínez, Chapter 1 – The Power of Ultrasound, J.-L. Capelo-Martínez, Ed., Ultrasound in Chemistry: Analytical Applications, WILEY-VCH Verlag GmbH & Co. KGaA, Weinheim, 2009.
[43] Y. Zhang, L. Ye, W.G. Zhao, L.L. Chen, M. Zhang, G. Yang, H.W. Zhang, Antifouling mechanism of the additive-free β-PVDF membrane in water purification process: relating the surface electron donor monopolarity to membrane-foulant interactions, J. Membr. Sci., 601 (2020) 117873–117883.
[44] X. Li, J.S. Li, X.F. Fang, K. Bakzhan, L.J. Wang, B. Van der Bruggen, A synergetic analysis method for antifouling behavior investigation on PES ultrafiltration membrane with self-assembled TiO_2 nanoparticles, J. Colloid Interface Sci., 469 (2016) 164–176.
[45] R. Field, Chapter 1 – Fundamentals of Fouling, K.-V. Peinemann, S. Pereira Nunes, Eds., Membrane Technology: Volume 4: Membranes for Water Treatment, WILEY-VCH Verlag GmbH & Co. KGaA, Weinheim, 2010.